Paper ID APEN-MIT-2022_8442
Applied Energy Symposium: MIT A+B
July 5-8, 2022 • Cambridge, USA

A Full-Scale Experimental Investigation of an Advanced Geothermal Energy Storage System

Josiane Jello
Department of Civil and Environmental Engineering
University of Illinois at Urbana-Champaign
Urbana, United States
jjello2@illinois.edu

Tugce Baser
Department of Civil and Environmental Engineering
University of Illinois at Urbana-Champaign
Urbana, United States
tbaser@illinois.edu

Abstract— This paper focuses on development of a full-scale heat injection experiment to investigate the feasibility of an Advanced Geothermal Energy Storage (AGES) system using an existing oil well in Illinois. AGES systems hold a significant potential to provide renewable and sustainable energy development and decarbonizing the oil and gas industry. The field experiment included sealing of the well and injection of a heated brine into the targeted heat storage formation. Temperature data were collected during the experiment using a Distributed Temperature Sensing (DTS) system and were analyzed over a period of 15 days. The results are interpreted and presented. The results indicate that implementing an AGES system is feasible.

Keywords—geothermal energy, abandoned hydrocarbon wells, heat storage, distributed temperature sensing

I. Introduction

An Advanced Geothermal Energy Storage (AGES) system present a solution for developing a geothermal system in areas where the subsurface temperature and geothermal gradient are relatively low compared to the traditional geothermal reservoirs. It functions by injecting heat from different sources, such as excess heat from renewable energy and industrial processes into the subsurface to create an artificial geothermal reservoir. The stored heat in the subsurface can be utilized for direct heating and cooling or electricity generation. Fig. 1 illustrates a schematic for the proposed AGES system.

Field experiments, laboratory investigations, and numerical analysis are needed to understand and quantify the thermal characteristics of the targeted reservoir to better design for an AGES system. Studies have been performed to determine the effect of both the thermal and hydraulic properties of the storage performance and efficiency of a reservoir and focused on sedimentary basins. A parametric analysis is performed to identify the desirable characteristics such as permeability, permeability heterogeneity, porosity, reservoir thickness, and injection rates. Results shows that the permeability affect the induced pressure due to the injection operations. Permeability heterogeneity and porosity have little effect on the system's performance. The thickness of the reservoir affects the thermal front evolution, where the temperature will advance farther for a thinner formation. Regarding the flow rate, the thermal front will move farther for a high injection flow rate [1, 2, 3]. Similar studies are also performed, and the results are consistent with these findings [4, 5]. Other studies showed that the system is suitable for long-term seasonal storage and almost all heat can be fully recovered [6, 7].

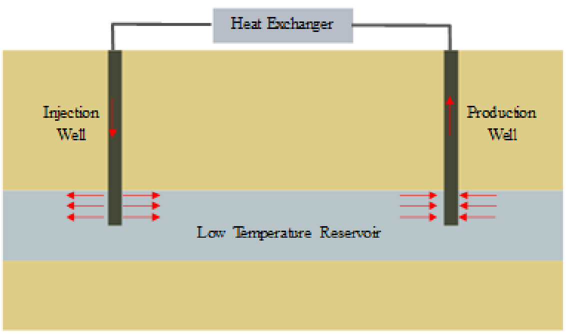

Figure 1. Conceptual schematic of an AGES system

The economic feasibility of utilizing sedimentary basins to store thermal energy have been investigated. The levelized cost of electricity (LCOE) calculated us $0.13/kWhe [4]. Another study performed a techno-economic analysis and the levelized cost of storage (LCOS) was cheaper than existing seasonal storage systems and is ¢12.4/kWhe for 4,000 h seasonal storage.

This paper presents and discusses the results of a full-scale field experiment analysis on an AGES system in the low temperature Illinois basin utilizing abandoned oil and gas wells to investigate the feasibility of installing such systems.

II. Well Site Selection

The M. Eckleberry #4 well site is selected after analyzing and interpreting existing data from abandoned hydrocarbon wells in the Illinois basin as shown in Fig. 2 to perform the field test. The well was scheduled to be plugged and abandoned, but the oil company was able to reduce the cost associated with the plugging and abandoning by providing the well for the field test. The surface infrastructure of the site is evaluated for suitability.

The well drilling was completed on August 22, 2013, and extends 958 meters into the subsurface. Well logging tools including Cement Bond Log, Casing Collar Locator, and Gamma Ray are utilized to assess the cement conditions between the well casing and rock formations and identify the different formations along the well depth.

To select a suitable reservoir for thermal energy storage, petrophysical, thermal, and hydraulic properties from existing well data were analyzed. Based on the analyses, Cypress Middle formation was selected.

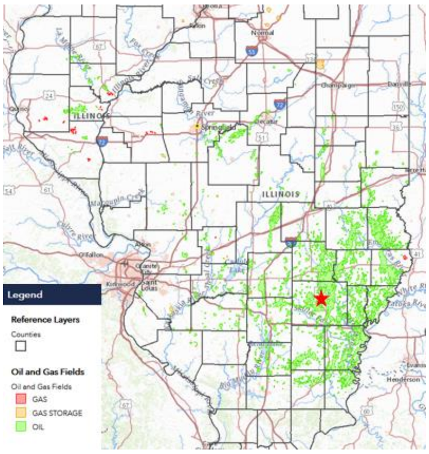

Figure 2. Location of M. Ecklberry well site in the southern Illinois basin

III. Field Test

The field test was performed to evaluate the thermal energy storage characteristics of the selected reservoir. The test consists of four phases: (1) hot fluid injection, (2) thermal decay monitoring, (3) cold fluid injection, and (4) thermal decay and pressure fall off. Fig. 3 (a) illustrates a schematic of the test performed.

The field preparation and setup included mobilizing a frac tank with fresh water installed near the well, a generator, a flow pump, and a heater. The perforation interval spans between 901.5 m and 903 m. To perform this operation, a perforation gun loaded with 21 grams of deep penetrating titan charges was used. Additionally, fluid samples are collected and tested for alkalinity, hydrogen sulfide (H_2S), total dissolved solids (TDS), density, and pH. Also, the well is instrumented with a distributed sensing temperature (DTS). the fiber optic cable was spliced and secured in the downhole housing assembly. In addition, a pressure/temperature memory gauge was added to the downhole assembly. All components were measured and the DTS cable was deployed in the hole as shown in Fig. 3 (b). Furthermore, the interrogator was set up and Silixa software was installed on the site computer.

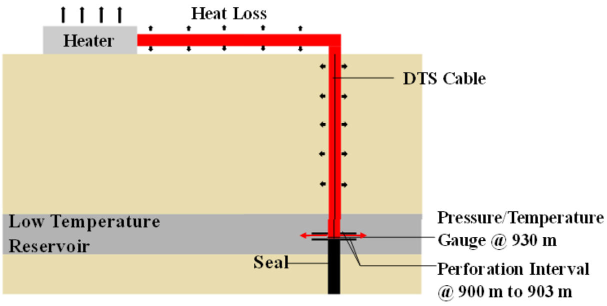

(a)

(b)

Figure 3. (a) Schematic of the field test (b) instrumentation installation in the well

The heat injection test began by setting up the components such as insulated flow lines, line heater and well head as shown in Fig. 4 (a) and (b). Two pressure gauges and a flow meter were also installed. Also, a wireless pressure gauge was placed on the line heater. Hot water injection into the well than started on April 5, 20201 at a rate of 8 gpm and temperature of 50 ℃. After 3 days of injection, the well was shut in and pressure fall off was monitored. After that, the thermal decay and pressure fall off were monitored for five days prior to the cold-water injection test was initiated and lasted for three days. The operation began by injecting fluid at a rate of 2 gpm for 3 hours, then it was ramped up to 4 gpm for an additional 3 hours. Then, an increase to 6 gpm was applied for the remaining volume of fresh water in the frac tank. After that, the cold-water injection was stopped, thermal decay and pressure fall off was performed and spanned for 18 days, ending the field experiment on May 5, 2021.

(a)

(b)

Figure 4. (a) Flowlines and wellhead insulation (b) line heater for hot water injection

IV. Field Test Results

The temperature data were collected using the DTS system. The DTS technology uses a fiber optic cable as a temperature sensor and records measurements capable of capturing the borehole's spatiotemporal temperature dynamics. The technology sends light pulses down the cable along the wellbore and the signal return time is recorded and correlated to the temperature at a certain depth. The interpretation utilizes Raman backscattering signal that is composed of Stokes and Anti-Stokes frequency bands that are dependent on temperature [8].

A. Initial Temperature Profile

Prior to the beginning of the field test, the temperature was recorded using the DTS system. The data is reported in Fig. 5 and the geothermal gradient is calculated.

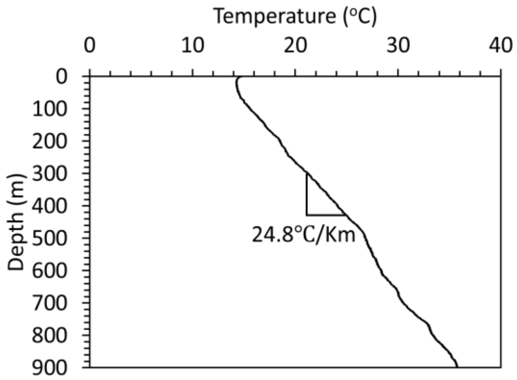

Figure 5. Initial basin temperature prior to field test

B. Temperature Profiles

The temperature profiles are plotted for the 4 phases of the field experiment. The temperature change along the depth is interpreted to better understand the system's performance. The hot fluid injection test lasted from April 5 to April 8, 2021. As shown in Fig. 6, the subsurface gained heat up to 500 m, where the recorded temperature is higher than the initial. Beyond that depth, the temperature recorded is recorded, indicating that the heat injected dissipated to the upper layers.

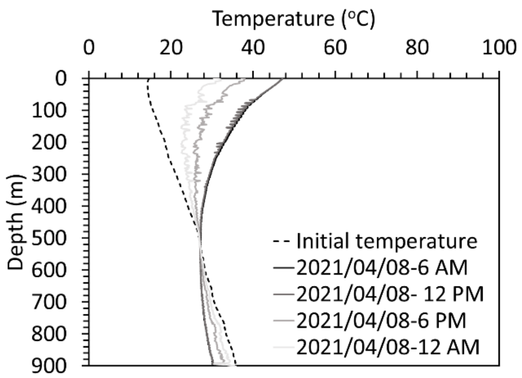

Figure 6. Temperature profile on April 8, 2021

The thermal decay and pressure fall off lasted from April 9 to 14, 2021. During this phase, the temperature profile approached the initial temperature and as shown in Fig. 7.

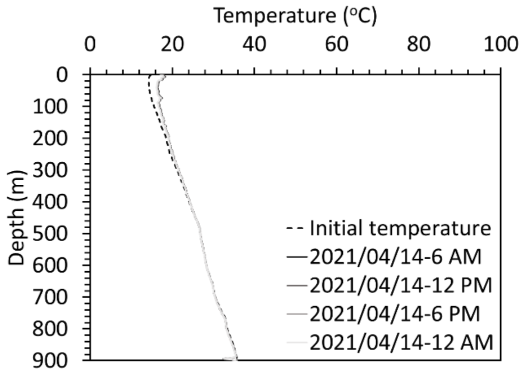

Figure 7. Temperature profile on April 14, 2021

After reaching equilibrium, the cold fluid injection started and lasted from April 15 to 16, 2021 as shown in Fig. 8. At the shallow formations, the temperature did not vary by much as compared to the initial temperature. At deeper depths, the formations are more affected by the cold-water injection.

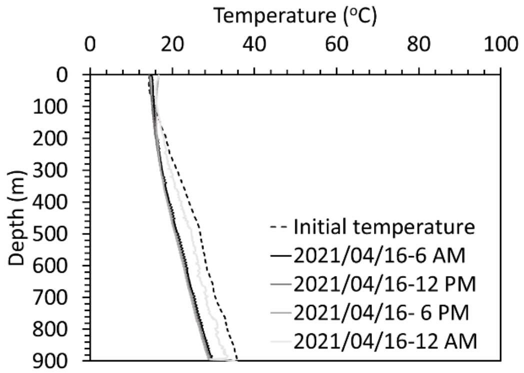

Figure 8. Temperature profile on April 16, 2021

Following phase 3, the rate of thermal decay and pressure fall off are monitored. The temperature profile approached the initial temperature profile.

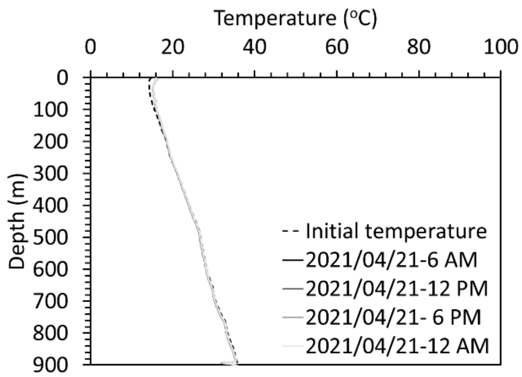

Figure 9. Temperature profile on April 21, 2021

C. Temperature Time Series Plots

The temperature time series are shown in Fig. 10(a) through 10(d) for depths 300 m, 500 m, 700 m, and 900 m. The different phases outlined correspond to the field test phases listed above.

An increase in temperature was recorded during phase 1, indicating that heat is transferred from the fluid to the surrounding. At depth 300m (Fig. 10a), the rate of heating recorded is higher than that at depth 500 m (Fig. 10b). On the other hand, at depths 700 m and 900 m (Fig. 10c and 10d), cooling during the heating phase is recorded, which is consistent with the temperature profile recorded (Fig. 6). As for phase 3, cooling was observed for all depths. The rate of cooling was higher for deeper depths. This phenomenon observed is attributed to the relatively injection flow rates and temperature. The selection of the injection flow rate was limited to the available equipment with the given budget and to the limited information on the mechanical properties of the formation, thus preventing fracturing of the rock. However, the data collected helped better understand the thermal and storage characteristics of the reservoir.

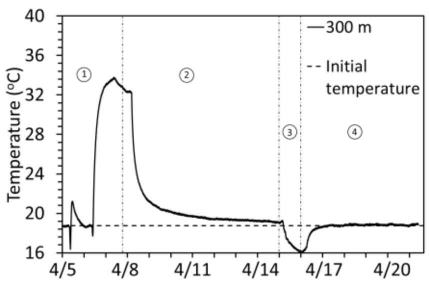

(a)

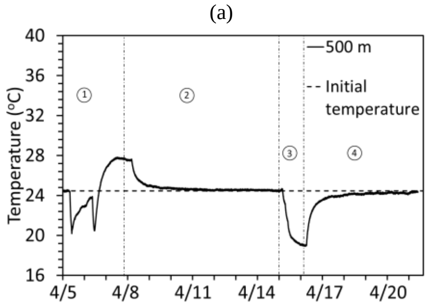

(b)

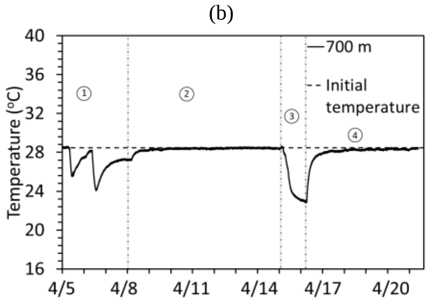

(c)

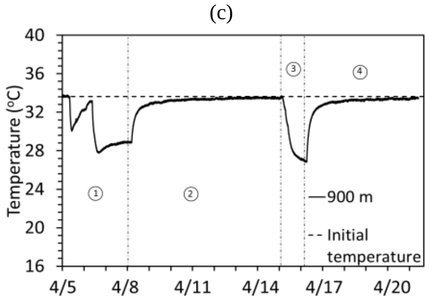

(d)
Figure 10. Temperature time series at (a) 300 m (b) 500 m (c) 700 m (d) 900 m

D. *Temperature Heatmap*

The temperature distribution throughout the field test is shown in Fig. 11. From the heat map, the different stages of the field experiment are delineated and observed. With hot water being injected on April 5 for 3 days, higher temperatures can be observed on shallow formations. Cooling is observed surrounding the injection region at greater depths due to the cooling of nearby formations. During the first thermal decay period, the residual heat from the injection is retained, with shallower depths having greater heat retention. On April 15, the effect of cold-water injection is denoted by the lower temperature around 16°C that narrows down with increasing depth as surrounding formation heats the injected water. Compared to the thermal decay of hot-water injection, the thermal stability of the cold-water injection occurs more rapidly, and its effects also did penetrate deeper into the well.

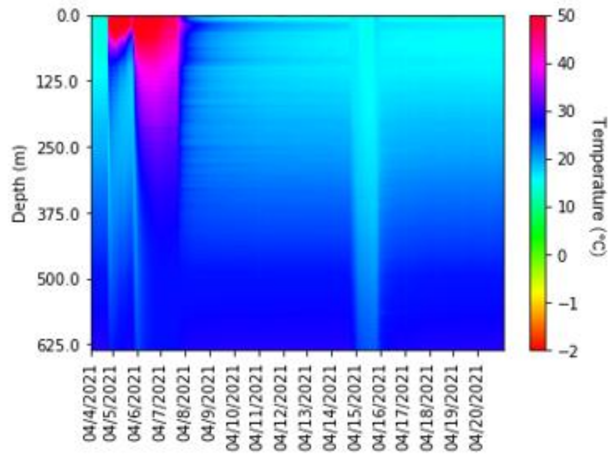

Figure 11. Heat map for temperature distribution throughout the field experiment

V. Discussion

The procedure presented offers a reliable method for converting an oil and gas well into a thermal storage well. The available petrophysical and geologic data helps in the site and reservoir selection and saves operational costs.

The heat losses in the well were higher than expected, which explains the cooling recorded at deeper depths and not reaching the intended reservoir. This was attributed to the limited budget of the project. Selecting a shallower formation would also have reduced the heat losses and reduced the operational costs.

The selected site did not have municipal water and electricity. A site with easier access to water and electricity can save the operator operation costs. Additionally, early planning for weather conditions is important.

VI. Conclusion

This paper focuses on the field experiment performed in the low temperature Illinois Basin for an advanced geothermal energy storage system using an existing oil and gas well. The available petrophysical and geologic data from were analyzed and helped in accelerating the selection of the site and reservoir process. The field test consisted of four phases, including a hot water injection phase, cold water injection phase, and two thermal decay and pressure fall off phases.

The operational parameters, including the injection rate and temperature, is critical to reduce the heat losses to the surrounding and to prevent any fluid within the rock formation of mixing with the injected fluid.

Even though heat losses were recorded, the data generated will assist for further studies. A numerical model will be developed and calibrated with the data collected, from which different injection scenarios with different operational parameters will be tested to better understand the heat storage characteristics, performance, and long-term efficiency.

Acknowledgment

Funding from Department of Energy is much appreciated. The opinions are those of the authors alone and do not reflect the viewpoint of the sponsor.

References

[1] Panja, P., McLennan, J., & Green, S. (2020, June). Temperature and Pressure Profiles for Geothermal Battery Energy Storage in Sedimentary Basins. In 54th US Rock Mechanics/Geomechanics Symposium. OnePetro.

[2] Panja, P., McLennan, J., & Green, S. (2021a). Impact of permeability heterogeneity on geothermal battery energy storage. Advances in Geo-Energy Research, 5(2), 127-138.

[3] Panja, P., McLennan, J., & Green, S. (2021b). Influence of permeability anisotropy and layering on geothermal battery energy storage. Geothermics, 90, 101998.Geothermal Technologies Office, US DOE. (2019) “GeoVision: Harnessing the Heat Beneath Our Feet - Analysis Inputs and Results.” United States. https://doi.org/10.15121/157236

[4] Wendt, D. S., Huang, H., Zhu, G., Sharan, P., McTigue, J., Kitz, K., ... & Neupane, G. H. (2019). “Flexible Geothermal Power Generation utilizing Geologic Thermal Energy Storage: Final Seedling Project Report “ (No. INL/EXT-19-53931-Rev000). Idaho National Lab.(INL), Idaho Falls, ID (United States).Tester, J. W., Herzog, H. J., Chen, Z., Potter, R. M., & Frank, M. G. (1994). Prospects for universal geothermal energy from heat mining. Science & Global Security, 5(1), 99-121.

[5] Zheng, Q. (2014). Design of a High Temperature Subsurface Thermal Energy Storage System. Clemson University.

[6] Green, S., McLennan, J., Panja, P., Kitz, K., Allis, R., & Moore, J. (2021). Geothermal battery energy storage. Renewable Energy, 164, 777-790.

[7] Neupane, Ghanashyam. Dynamic Earth Energy Storage: Terawatt-Year, Grid-Scale Energy Storage using Planet Earth as a Thermal Battery (GeoTES): Seedling Project Final Report. United States. https://doi.org/10.15121/163871

[8] Mawalkar, S., Brock, D., Burchwell, A., Kelley, M., Mishra, S., Gupta, N., ... & Shroyer, B. (2019). Where is that CO2 flowing? Using Distributed Temperature Sensing (DTS) technology for monitoring injection of CO2 into a depleted oil reservoir. International Journal of Greenhouse Gas Control, 85, 132-142.